IL NUOVO CIMENTO Vol. 34 C, N. 5 Settembre-Ottobre 2011
DOI 10.1393/ncc/i2011-10962-2

Communications: SIF Congress 2010

Phonon replicas lineshape in GaN epilayers: The A and B exciton contributions

L. Cavigli

*Dipartimento di Fisica e Atronomia, Università di Firenze - via G. Sansone 1
50019 Sesto Fiorentino (FI), Italy*

(ricevuto il 28 Dicembre 2010; approvato il 30 Dicembre 2010; pubblicato online il 19 Settembre 2011)

Summary. — A thorough investigation of the lineshape of phonon-assisted emission in a high-quality *c*-plane GaN epilayer is presented up to 200 K. Before addressing the lineshape analysis, we corrected distortions in the phonon replica spectra due to etaloning effects, by performing photoluminescence and reflectivity measurements. The comparison with existing models for phonon replicas shows that the commonly adopted description of the exciton-phonon interaction involving a single excitonic band leads to a large discrepancy with the experimental data. Only the consideration of the complex nature of the excitonic band in GaN, including A and B exciton contributions, allows accounting for the temperature dependence of phonon replicas lineshape.

PACS 78.55.-m – Photoluminescence, properties and materials.
PACS 78.55.Cr – III-V semiconductors.
PACS 71.35.-y – Excitons and related phenomena.
PACS 71.38.-k – Polarons and electron-phonon interactions.

1. – Introduction

Exciton-phonon coupling is a fundamental interaction occurring in semiconductors, both bulk and nanostructures, which strongly affects their optical and electrical properties [1, 2]. Different mechanisms, such as Fröhlich interaction, deformation and piezoelectric potentials, rule the exciton-phonon interaction and the investigation of these phenomena gives important insights on the relaxation, thermalization and transport properties of carriers.

Usually the exciton-phonon interaction is stronger in ionic II-VI semiconductors, with respect to the nearly covalent III-V compounds [1]. A remarkable effect of this interaction is the presence, in II-VI materials, of intense phonon replicas (PRs) of the excitonic emission, which are almost missing in GaAs and similar materials. At low temperatures, excitonic recombination in high-quality ionic materials consists in the main radiative free-exciton recombination lines (the so-called zero phonon lines (ZPL)) and their PRs separated by an energy spacing close to $\hbar\omega_{LO}$ (corresponding to the longitudinal optical phonon energy). The PR spectra not only contain information on the different mechanisms ruling the exciton-phonon interaction, but they are also a useful tool for investigating the exciton recombination kinetics and the corresponding density of states. Therefore the PR lineshape and intensity have been indeed the subject of thorough experimental and theoretical investigations in different semiconductor materials and nanostructures [1, 2].

Among III-V semiconductors, III-nitrides are unusual in so far as they exhibit a large ionic character and in fact PRs are a common feature of excitonic recombinations occurring in GaN-based systems [2]. Different models have been proposed to reproduce the PR features: initially a configurational model has been considered to extract the Huang-Rhys factor [3, 4] from the ratio of the intensity of the replicas which arise from the radiative recombination of excitons assisted by the emission of n phonons. The analysis of PRs originating from strongly localized excitons, or excitons bound to defects was satisfactorily interpreted in the framework of this model [5, 6].

Only recently the quality of wurtzite GaN epilayers has been greatly improved and the free-exciton recombination can prevail over the bound-exciton recombination even at low temperature. Clear features arising from the A and B exciton recombinations have been reported in the zero-phonon line photoluminescence (ZPL-PL) of GaN epilayers [7,8] and even in quantum wells [9,10]. This has made possible the comparison with models where the intrinsic nature of the exciton is considered. Detailed investigations have been already reported concerning the phonon-induced thermal broadening of the excitonic lines and the main characteristics of the phonon-assisted emission [11]. Until now, most of the experimental studies on spectral shift [12-16], intensity [17-19] and lineshape [20, 13, 18, 19,15,16,21,8] of PRs emission with temperature (T) have been performed in a restricted T range ($T < 100\,\mathrm{K}$) and the corresponding data have been systematically modeled by neglecting the B exciton contribution. A close analysis of the reported data, mainly those at higher T concerning of PR spectral shift [12, 16] and lineshape [15, 12, 16, 13, 21, 19], evidences only a poor agreement with the model predictions. Only few studies analyzed the spectral lineshape, ascribing discrepancies with the model to the presence of residual impurity scattering [21].

Recently, an analysis of PRs emission in an extended temperature range has been reported [22], where the 1LO- and 2LO-phonon emission have been compared with the commonly accepted model [23, 24], showing that to fully reproduce the PRs spectral shift in the whole investigated temperature range, both the A and B excitonic bands have to be taken into account.

In this paper, a detailed analysis of 2LO PRs lineshapes as a function of temperature (up to 200 K) of a high-quality non intentionally doped (*nid*) GaN epilayer grown on a *c*-plane sapphire substrate is reported. We clearly show that, to fully reproduce the experimental spectra, both the A and B excitonic bands have to be taken into account, proving a very satisfactory agreement with the theoretical model when the complexity of the GaN valence band is considered.

2. – Experimental details

The investigated sample is a $3\,\mu\mathrm{m}$ thick *nid* wurtzite GaN epilayer grown by metal organic vapor phase epitaxy (MOVPE) on a *c*-plane sapphire substrate characterized by a threading dislocation density lower than $1 \times 10^9\,\mathrm{cm}^{-2}$. All measurements were performed

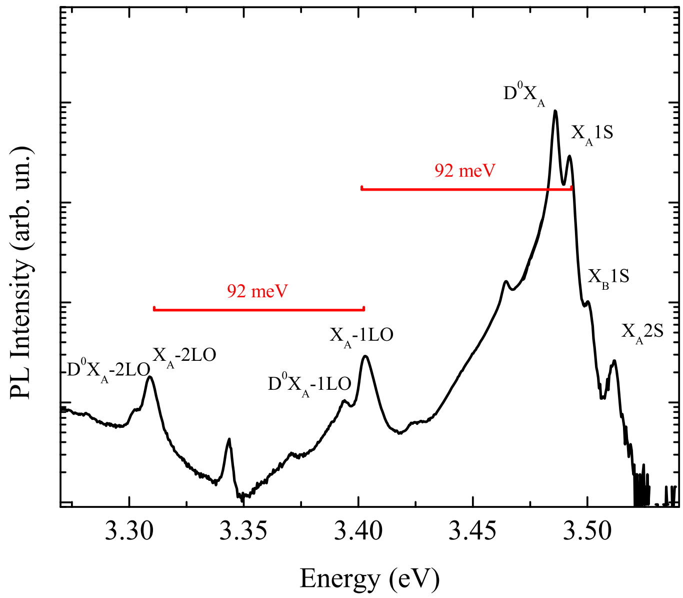

Fig. 1. – PL spectrum (semi-log scale) at 10 K. The ZPL and PRs emission are highlighted.

with the sample placed in a closed-cycle cryostat, ranging the temperature between 10 K and 200 K. Reflectivity (R) measurements at normal incidence were carried out using a CW Xe lamp. Time-integrated photoluminescence (TI-PL) measurements were performed under nonresonant excitation by a frequency-doubled dye laser (wavelength 300 nm). R and PL experiments probed the same sample portion to ensure a careful and systematic analysis of the bandedge properties. In both cases, the collected light was detected by a cooled silicon CCD after dispersion through a 50 cm flat field spectrometer offering a spectral resolution of 0.5 meV.

3. – Discussion

In fig. 1, a typical PL spectrum is shown at 10 K, where are clearly evidenced the ZPL and PRs emission. The main spectral features observed in the ZPL at 10 K are related to a neutral donor-bound exciton recombination (D^0X_A) and to the X_A and X_B exciton radiative recombinations. The emission from the 2S state of X_A excitons is also detected at higher energy. Fitting the ZPL with a Gaussian lineshape allows to extract an inhomogeneous broadening of the X_A emission band of 1.5 meV HWHM, indicating the high quality of the epilayer and its excellent strain homogeneity, corresponding to a biaxial stress variation of ± 1.0 kbar [25]. The energy separation between the excitonic resonance X_B and X_A, derived from the reflectivity spectra (not shown), is $E_{X_B} - E_{X_A} = 8.0 \pm 0.5$ meV, in agreement with the values reported in the literature for GaN epilayers grown on *c*-plane sapphire [7]. The PRs at 10 K are also highlighted in fig. 1. Phonon-replicas of D^0X_A and X_A states are observed for the first and second order. An energy separation of $\hbar\omega_{LO} = 92 \pm 0.5$ meV is measured between the D^0X_A state and its 1LO-phonon replica, in agreement with Raman spectroscopy and Inelastic X-Ray scattering results [26-28].

We want to focus our attention on the dependence of the PRs lineshape on temperature. According to the established theory [23,24], the intensity of the n-th phonon replica for a thermalized exciton distribution turns out to be given as

$$I_n(E_X + E_k - n\hbar\omega_{LO}) \approx \mathrm{W}_n(E_k)\rho(E_k)e^{-\frac{E_k}{k_B T}}, \quad (1)$$

where E_X is the ZPL transition energy, E_k is the exciton center-of-mass kinetic energy, $\rho(E_k)$ indicates the exciton density of states (DOS), $\mathrm{W}_n(E_k)$ is the energy-dependent probability that an exciton with kinetic energy E_k recombines emitting n-phonons and T is the excitonic temperature. In the framework of a perturbative approach to describe the exciton-phonon interaction, W_n depends linearly on the energy E_k for 1LO replica and it is energy-independent for 2LO replica, as a consequence of energy and momentum conservation [23, 24]. The emission probability in eq. (1) is weighted by the Boltzmann factor which accounts for a thermalized nondegenerate exciton distribution. If we consider an ideal bulk sample we should therefore expect that different PRs have distinctive features related to the density of states and the matrix element. In particular, different spectral shapes are expected for the 1LO and 2LO-phonon emission.

As already discussed in [22], due to etaloning effects (see the modulation observed in the reflectivity spectra, fig. 2a and b) in the transparent region of PR emission, any direct comparison of PR-PL data with theoretical models, concerning either the peak position or the lineshape, cannot be based on measured spectra, as usually done in the literature, in particular for high temperatures. In fact, while at low temperatures the reflectivity spectrum in the PR spectral region shows a modulation with a period much larger than the full width half maximum of the PR lines (fig. 2a) and the experimental PR lineshapes are independent of the investigated point of the sample, when increasing the temperature we observe a structuring of the replica lineshapes, as shown in fig. 2b, where data at $T = 140\,\mathrm{K}$ are reported. Different PR lineshapes are found for different points in the sample, denoting a spatially dependent nature of the PR structuring (possibly related to local variation of the sample thickness and/or strain-induced refraction index changes), while the ZPL lineshape (not reported here) does not change when probing different spatial regions of the sample. Note that even the energy of the maximum of the PR band is position-dependent. The appearance of structures in the replicas, as the thermal broadening gets important, is an artifact caused by the etaloning effect, as clearly shown by the reflectivity spectra. In fact, in the spectral region where very weak absorption is present, we observe a strong modulation both in the reflectivity and PL signals, with a coincidence of the modulation spacing observed in both R and PL spectra. Given the energy scale of the interference pattern, the modification of the PR lineshape gets more important as $T \geq 80\,\mathrm{K}$, when the PR band becomes broad, requiring an appropriate correction before comparing the experimental PR lineshape and PR energy peak position with any theoretical model [23, 24] in the high-temperature range.

Following the same procedure described in ref. [22] to correct the PR lineshape, we consider the sample acting as a spectral filter for the luminescence below the energy bandgap. Therefore, we define a transfer function $TF(E)$ between the internal PL and the external (measured) PL. Since in the spectral region of interest the absorption is negligible, $TF(E)$ is proportional to the transmittivity $T(E)(TF(E) \propto T(E) = 1-R(E)$, $R(E)$ being the reflectivity). In the absence of an absolute value of the reflectivity we can correct the PL intensity using the following phenomenological expression:

$$I_{PL}^{Corr}(E) = \frac{I_{PL}(E)}{TF(E)} = \frac{I_{PL}(E)}{1 - \gamma R^{Exp}(E)}, \quad (2)$$

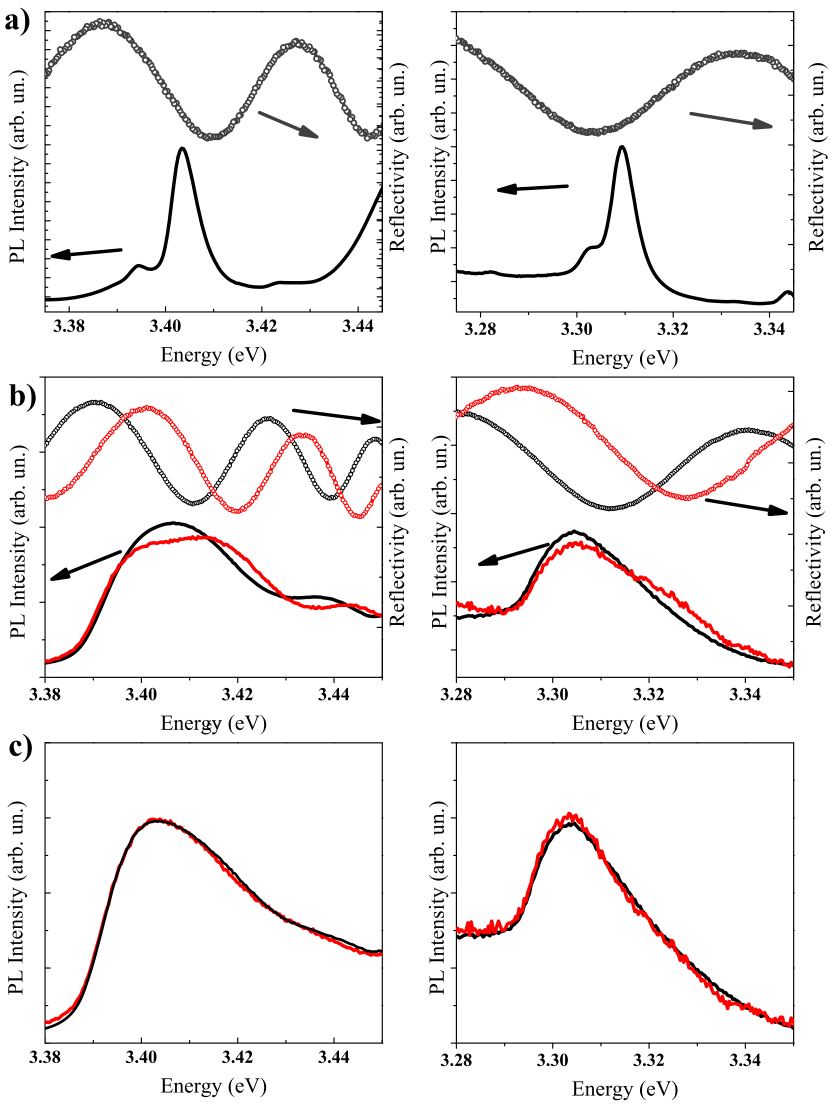

Fig. 2. – (Color online) On the left-hand side: 1LO-PL spectra measured at (a) $T = 10\,\text{K}$ and (b) $T = 140\,\text{K}$ and their corresponding reflectivity spectra (open symbols), (c) the same spectra (at $T = 140\,\text{K}$) of (b) displayed after correction with eq. (2). On the right-hand side: 2LO-PL spectra measured at (a) $T = 10\,\text{K}$ and (b) $T = 140\,\text{K}$ and their corresponding reflectivity spectra (open symbols), (c) the same 2LO-PL spectra (at $T = 140\,\text{K}$) on (b) displayed after correction with eq. (2). The two set of measurements in (b) e (c) refer to two different points on the sample (a given color refers to a given position on the sample).

where $R^{Exp}(E)$ is the experimental reflectance spectrum detected from the same spot than the PL one and γ is a constant fitting parameter $(R(E) = \gamma R^{Exp}(E))$. PL spectra corrected using eq. (2) are reported in fig. 2c and the corrected PR spectra (1LO on the right-hand side and 2LO on the left-hand side) exhibit the same structureless lineshape, independent of the probed spatial region. The reconstruction of an intrinsic lineshape

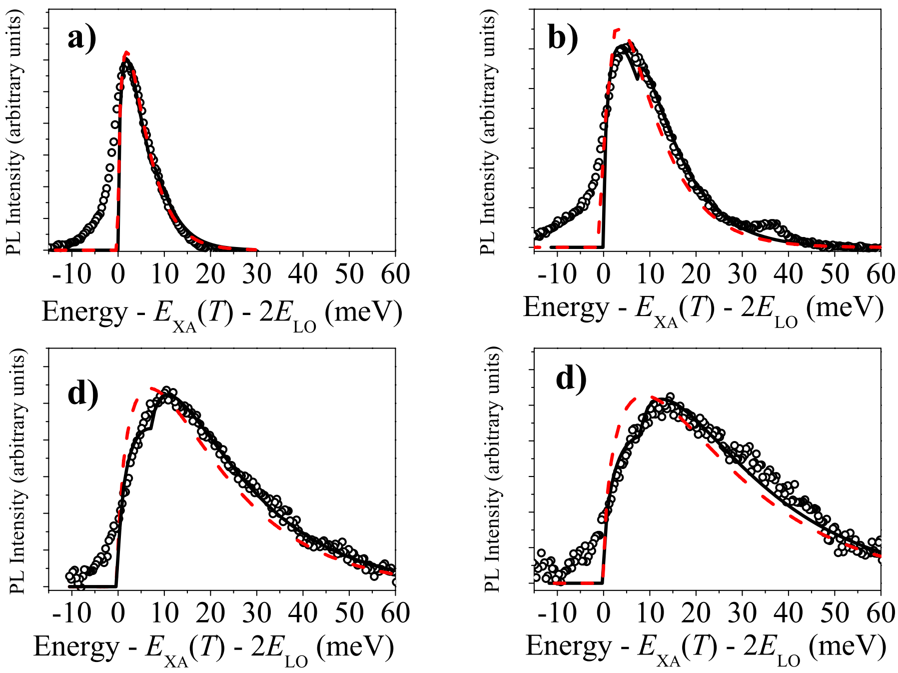

Fig. 3. – (Colour online) 2LO-PL spectra (a) at 40 K, (b) at 80 K, (c) at 160 K and (d) at 200 K. Open circles refer to experimental spectra, red dashed lines refer to fit to the data considering only the A exciton band contribution, with the phonon energy of 92 meV as a fixed parameter, black solid lines refer to fit to the data considering the A+B exciton band contribution, with the phonon energy of 92 meV as a fixed parameter.

for the PR spectra allows us to perform an accurate study of their lineshape in a wider temperature range, as compared with previous studies.

In previous studies the 2LO phonon replica linewidth Γ has been studied as a function of temperature and compared with the common model [23, 24], which predicts, within a single exciton band description, $\Gamma_{2\mathrm{LO}} = 2.96 k_B T$ [19]. We then analysed our 2LO PR emission lineshapes, after etaloning correction, with eq. (1) in an extended temperature range. For $n = 2$, eq. (1) becomes

$$I_2(E_X + E_k - 2\hbar\omega_{LO}) = A(E_k)^{\frac{1}{2}} e^{-\frac{E_k}{k_B T}}. \tag{3}$$

We fit the data to eq. (3), setting the phonon energy at 92 meV (as experimentally measured), the experimental value for temperature, and A the only free parameter. Best fits are reported in fig. 3, dashed lines, for data at 40 K (fig. 3a), 80 K (fig. 3b), 160 K (fig. 3c) and 200 K (fig. 3d). The single-band model [23, 24] reproduces the experimental lineshape only for data at 40 K, while a clear deviation from the model is observed at higher temperatures. In order to overcome the observed discrepancy, we follow the analysis reported in [22], correcting the excitonic density of states $\rho(E_k) \propto \sqrt{E_k}$ taking into account the well-known presence of different excitonic states in the wurtzite GaN system. The C exciton can be neglected in the T range considered here, but, as reported in [22], the B exciton band becomes significantly populated as the temperature is greater than a few tens of kelvin. Such population will also play a role in the phonon-assisted emission, even though no clear band structuring is observed at high temperature in the PRs, besides the etaloning effects. By considering the presence of the B excitonic band, the theoretical function to be compared with the data in fig. 3, is

$$(4) \qquad I_2(E_{\mathrm{X_A}} + E_k - 2\hbar\omega_{LO}) = Ae^{-\frac{E_k}{k_B T}} \left[(E_k)^{\frac{1}{2}} + c_2(E_k - E_{\mathrm{X_B}} + E_{\mathrm{X_A}})^{\frac{1}{2}}\right],$$

where $E_{\mathrm{X_A}}$ and $E_{\mathrm{X_B}}$ are the energies of A and B excitons at $k = 0$. The factor c_2 accounts for the different exciton masses in the A and B bands. From the values reported in the literature [8] c_2 has been fixed to 0.5. In order to fit the experimental data of fig. 3 with eq. (4) the only parameter is A, all the other quantities, $E_{\mathrm{X_B}}$, T and phonon energy, being experimentally determined. In fig. 3, the experimental results are compared with the fits obtained considering both the A and B bands (black solid line) with no contribution of inhomogeneous broadening (HWHM = 1.5 meV): the data nicely agree with theory, when both exciton states are considered, with a unique phonon energy of 92 meV, coincident with that of the donor replica. The discrepancy on the low-energy side comes from neglecting the inhomogeneous broadening.

The very satisfactory agreement of the experimental data with the two-bands model (black solid lines in fig. 3) implies a full reconstruction of PR lineshapes in the whole investigated T range.

4. – Conclusions

A detailed investigation of the phonon replica emission in a high-quality c-plane GaN epilayer is reported. We have proved that care has to be taken when analyzing the PR spectra, due to the presence of multiple interference effects. The simultaneous measurement of PL and R spectra allows the correction for etaloning effects and the reconstruction of the intrinsic PR lineshapes. The comparison with existing models to describe the PR lineshape shows that the complex nature of the exciton band in GaN has to be considered to fully account for the 2LO PR lineshapes at high temperature.

* * *

It is a pleasure to thank Prof. Franco Bogani, Prof. Massimo Gurioli and Prof. Anna Vinattieri for their contribution to this work. I wish to thank the group of Prof. Nicolas Grandjean and Dr. Raphaël Butté for providing the sample.

REFERENCES

[1] Klingshirn C. F., *Semiconductor Optics*, 3rd edition (Springer-Verlag, Berlin) 2007.
[2] Gil B., *Low-dimensional nitride semiconductors* (Oxford University Press, New York) 2002.
[3] Huang K. and Rhys A., *Proc. R. Soc. London A*, **204** (1950) 406.
[4] Smith M., Lin J. Y. *et al.*, *Appl. Phys. Lett.*, **70** (1997) 2882.
[5] Leroux M., Grandjean N. *et al.*, *J. Appl. Phys.*, **86** (1999) 3721.
[6] Kalliakos S., Zhang X. B. *et al.*, *Appl. Phys. Lett.*, **80** (2002) 428.
[7] Viswanath A. K., Lee J. I. *et al.*, *J. Appl. Phys.*, **84** (1998) 3848.
[8] Monemar B., Paskov P. P. *et al.*, *Phys. Status Solidi B*, **245** (2008) 1723.
[9] Stokker-Cheregi F., Vinattieri A. *et al.*, *Phys. Rev. B*, **79** (2009) 245316.
[10] Stokker-Cheregi F., Vinattieri A. *et al.*, *Phys. Rev. B*, **77** (2008) 125342.

[11] Zhang X. B., Taliercio T. *et al.*, *J. Phys.: Condens. Matter*, **13** (2001) 7053.
[12] Wojdak M., Wysmołek A. *et al.*, *Phys. Status Solidi B*, **216** (1999) 95.
[13] Song D. Y., Basavaraj M. *et al.*, *J. Appl. Phys.*, **100** (2006) 113504.
[14] Zu S. J., Liu W. *et al.*, *Appl. Phys. Lett.*, **77** (2000) 3376.
[15] Xu S. J., Li G. Q. *et al.*, *J. Appl. Phys.*, **99** (2006) 073508.
[16] Buyanova I. A., Bergman J. P. *et al.*, *Solid State Commun.*, **105** (1998) 497.
[17] Liu W., Li M. F. *et al.*, *Semicond. Sci. Technol.*, **13** (1998) 769.
[18] Tkachman M. F., Shubina T. V. *et al.*, *Semiconductors*, **37** (2003) 532.
[19] Xu S. J., Li G. Q. *et al.*, *J. Chem. Phys.*, **122** (2005) 244712.
[20] Kovalev D., Averboukh B. *et al.*, *Phys. Rev. B*, **54** (1996) 2518.
[21] Buyanova I. A., Bergamn J. P. *et al.*, *Mater. Sci. Eng. B*, **50** (1997) 130.
[22] Cavigli L., Gabrieli R. *et al.*, *Phys. Rev. B*, **82** (2010) 115208.
[23] Segall B. and Mahan G. D., *Phys. Rev.*, **171** (1968) 935.
[24] Permagorov S., *Excitons* (North-Holland Publishing Company, Amsterdam) 1982.
[25] Gil B. and Briot O., *Phys. Rev. B*, **55** (1997) 2530.
[26] Davydov V. Y., Kitaev Y. E. *et al.*, *Phys. Rev. B*, **58** (1998) 12899.
[27] Ruf T., Serrano J. *et al.*, *Phys. Rev. Lett.*, **86** (2001) 906.
[28] Zhang J. M., Ruf T. *et al.*, *Phys. Rev. B*, **56** (1997) 14399.